A study of Impinging Flow on a Rotating Disc

Horia DUMITRESCU[1], Vladimir CARDOS*,[1], Florin FRUNZULICA[1,2]

*Corresponding author
*,[1]"Gheorghe Mihoc – Caius Iacob" Institute of Mathematical Statistics and Applied Mathematics of the Romanian Academy
Calea 13 Septembrie no. 13, 050711 Bucharest, Romania
horiadumitrescu@yahoo.com, v_cardos@yahoo.ca*
[2]"POLITEHNICA" University of Bucharest, Faculty of Aerospace Engineering,
Polizu no.1-6, RO-011061, Bucharest, Romania
ffrunzi@yahoo.com

DOI: 10.13111/2066-8201.2014.6.3.5

Abstract: *This paper focuses on the behavior of the boundary-layer laminar flow produced by a large radius no-thickness disc which rotates inside an axial stream. Some early solutions are only known for the upstream flow field, but the details of the flow behind the disc are still obscure. A better understanding of the mechanisms and the properties of the shear layer close to disc is sought through the development of an analytic theory and then is completed by CFD computations. This article also shows that the basic flow on the leeward side of disc is mostly rotational-inviscid and only on in the neighborhood of the disc surface there is a viscous layer which rotates drawn by disc. The viscous layer containing a thin Ekman sublayer and a thicker essentially inviscid superlayer, governed by Taylor-Proudman theorem, can carry three possible actions: centrifugal (pumping) mode, neutral mode and centripetal (suction) mode. The action type depends on the relative importance of effects given by translation of the fluid (W) and rotation of the disc (ΩR), defined by a rotating parameter (W/ΩR). The existence of such modes is connected to the amount of angular momentum transferred outside the Ekman sublayer. A CFD analysis was used to identify the vortex structure which is responsible for the angular momentum transfer from the rotating disc to an axial stream.*

Key Words: *Boundary layer, Rotating disc, Similarity solutions, inviscid superlayer*

1. INTRODUCTION

One simple case of boundary layer on rotating body is the rotating disc in an initially stationary fluid, known also as the free disc [1], [2]. The solution is also a rare three-dimensional exact similarity solution of the Navier-Stokes equations [3]. The viscous stresses on the disc surface drag fluid elements near disc around in almost circular paths, and then centrifugal forces cause these elements to spiral outwards. The disc thus acts as a centrifugal fan with a radial flow component that has a wall-jet character directed away from the axis of rotation, whence the name of pumping effect. The fluid outwards thrown in this way is replaced by an axial flow directed towards the disc surface. The azimuthally flow component has a typical boundary-layer profile, monotonically increasing from zero at infinity to a constant value at the disc. The importance of this cross-flow structure is due to the inflexional cross-flow instability [4], which generates stationary vortices in many three-dimensional boundary layers of engineering interest.

Another simple case of typical three-dimensional boundary layer is the flow near a stationary disc, when the fluid at a large distance above it rotates at the constant angular

velocity [5]. When the fluid rotates over the wall, there is a similar effect with the first case but its sign is reversed: at large distance from the wall the outer rotational flow is governed by a balance between the centrifugal force and radial pressure directed towards the axis, while close to the wall the radial pressure unbalanced by the frictional retardation proceeds to drive the radial inward boundary-layer flow. For reasons of continuity, the motion then must be compensated by an axial flow upwards that has a wall-suction character, whence the name sucking effect.

The next problem is a disc of radius R rotating with an angular velocity Ω in an axial stream of velocity W_∞. Although this flow was before considered a simple extension of the previous cases [6], [7] it has been shown in reality to be more difficult [8].

Thus, the determination of the flow due to a rotating body of revolution (here a disc) immersed into a steady flow parallel to the axis of rotation of body is not a simple problem, and a clear picture of all aspects of the flow field is not yet available. This flow is governed by two parameters: Reynolds number $\mathrm{Re}_\Omega = \frac{\Omega R^2}{\nu}$, and the rotation parameter $\mu = \frac{W_\infty}{\Omega R}$, given by the ratio of free stream to tip velocity. The rotation parameter is a measure of the relative importance of the effects of uniform axial flow and the disc rotation. In the limit $\mu \to \infty$ and at infinity we may expect the velocity distribution to reduce to a uniform stream. At the other extreme, $\mu = 0$, it is plausible to meet again the flow around the free disc [1]. When μ is non-zero, the flow field in upstream of the disc appears to be broadly correct predicted in the past [6], [7]. But the details of the flow in the axially symmetric shear layer and the way the fluid moves behind the disc are obscure.

Generally, the physical origin of this flow is that the fluid in the boundary layer experiences centrifugal and wall shear stress forces, and these additionally act on the leeward side of the disc in an adverse pressure gradient, which can undergo separation. Thus the spiralling flow near the disc for $\mu \neq 0$ is presumably modified from the one for $\mu = 0$, although there is an all-or-nothing quality about the moving vortex structure which makes the nature of the modification difficult to imagine.

The new insights into the nature of the 3D boundary layer on the leeward side of the rotating disc and the vortex structures carrying angular momentum into fluid are derived and discussed.

2. PROBLEM FORMULATION

The basic flow for the disc rotating at constant angular velocity Ω_* in an otherwise still viscous incompressible fluid at kinematic viscosity ν_* (the asterisk subscript indicates a dimensional quantities) is obtained from the von Karman similarity solution [1]. Batchelor [9] showed that this flow is a limiting case of a family of flows with similarity solutions, in which both the disc and the fluid far from the disc rotate with different angular velocities: the Bödewadt layer [5], where the disc is stationary and the fluid rotate, and the Ekman layer [10], where the fluid and disc co-rotate at almost the same angular velocity. The similarity structure also persists for the present case when there is an axial flow towards the disc of velocity $W_{*\infty}$ [6].

Governing equations. We choose to work with cylindrical coordinates in a non-rotating frame of reference (Fig. 1). The axial and radial coordinates are z_* and r_*, respectively, the azimuthally angle is θ, time is t_*, and ρ_* is the density of the fluid. The velocities in the

radial, azimuthal and axial directions are u_*, v_* and w_*, respectively, and the pressure is p_*. The governing equations in an inertial frame are therefore

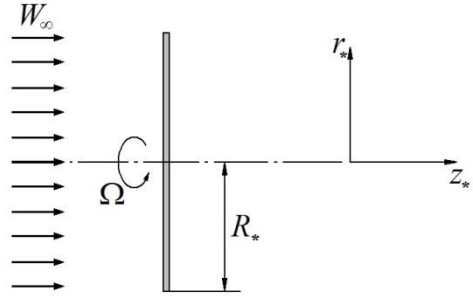

Figure 1 – Uniform superimposed flow of air impinging on the surface of rotating disc

$$\frac{1}{r_*}\frac{\partial\left(r_* u_*\right)}{\partial r_*}+\frac{1}{r_*}\frac{\partial v_*}{\partial\theta}+\frac{\partial w_*}{\partial z_*}=0, \tag{1}$$

$$D_* u_*-\frac{v_*^2}{r_*}=-\frac{1}{\rho_*}\frac{\partial p_*}{\partial r_*}+\nu_*\left(L_* u_*-\frac{u_*^2}{r_*^2}-\frac{2}{r_*^2}\frac{\partial v_*}{\partial\theta}\right), \tag{2}$$

$$D_* v_*-\frac{u_* v_*}{r_*}=-\frac{1}{\rho_* r_*}\frac{\partial p_*}{\partial\theta}+\nu_*\left(L_* v_*-\frac{v_*}{r_*^2}-\frac{2}{r_*^2}\frac{\partial u_*}{\partial\theta}\right), \tag{3}$$

$$D_* w_*=-\frac{1}{\rho_*}\frac{\partial p_*}{\partial z_*}+\nu_* L_* w_*, \tag{4}$$

where the differential operators are

$$D_*=\frac{\partial}{\partial t_*}+u_*\frac{\partial}{\partial r_*}+\frac{v_*}{r_*}\frac{\partial}{\partial\theta}+w_*\frac{\partial}{\partial z_*}, \tag{5a}$$

$$L_*=\frac{1}{r_*}\frac{\partial}{\partial r_*}\left(r_*\frac{\partial}{\partial r_*}\right)+\frac{1}{r_*^2}\frac{\partial^2}{\partial\theta^2}+\frac{\partial^2}{\partial z_*^2}, \tag{5b}$$

Equations 1-4 can be made dimensionless by dividing through by approximate parameters using the following transformations:

$$r_*=\left(\frac{\nu_*}{\Omega_*\sqrt{1+\mu^2}}\right)^{\frac{1}{2}} r, \tag{6a}$$

$$z_*=\left(\frac{\nu_*}{\Omega_*\sqrt{1+\mu^2}}\right)^{\frac{1}{2}} z, \tag{6b}$$

$$t_*=\frac{t}{\Omega_*\sqrt{1+\mu^2}}, \tag{6c}$$

Flow variables are separated into an axisymmetric steady basic flow, which respects von Karman's similarity structure and a more general unsteady part from [11], whose amplitude is characterized, by a small parameter $\varepsilon << 1$,

$$u_*\left(r_*,\theta,z_*,t_*\right)=r_*\Omega_*\left(1+\mu^2\right)^{\frac{1}{2}}U\left(z\right)+\varepsilon\left(\nu_*\Omega_*\sqrt{1+\mu^2}\right)^{\frac{1}{2}}\hat{u}\left(r,\theta,z,t\right), \tag{7}$$

$$v_*\left(r_*,\theta,z_*,t_*\right)=r_*\Omega_*\left(1+\mu^2\right)^{\frac{1}{2}}V\left(z\right)+\varepsilon\left(\nu_*\Omega_*\sqrt{1+\mu^2}\right)^{\frac{1}{2}}\hat{v}\left(r,\theta,z,t\right), \tag{8}$$

$$w_*\left(r_*,\theta,z_*,t_*\right)=\left(\nu_*\Omega_*\sqrt{1+\mu^2}\right)^{\frac{1}{2}}W\left(z\right)+\varepsilon\left(\nu_*\Omega_*\sqrt{1+\mu^2}\right)^{\frac{1}{2}}\hat{w}\left(r,\theta,z,t\right), \tag{9}$$

$$p_*\left(r_*,\theta,z_*,t_*\right)=\rho_*\nu_*\Omega_*\left(1+\mu^2\right)^{\frac{1}{2}}\left(P_z\left(z\right)+P_r\left(r\right)\right)+\varepsilon\left(\rho_*\nu_*\Omega_*\sqrt{1+\mu^2}\right)\hat{p}\left(r,\theta,z,t\right). \tag{10}$$

Substituting (6a)-(10) into (1)-(4) and equating terms of $\mathrm{O}\left(\varepsilon^0\right)$ gives the basic flow similarity equations

$$U^2+WU'-V^2=P'_r+U'', \tag{11}$$

$$U^2+WU'-V^2=P'_r+U'', \tag{12}$$

$$2UV+WV'=V'', \tag{13}$$

$$WW'=-P'_z+W'', \tag{14}$$

to be solved subject to boundary conditions,

$$U\left(0\right)=W\left(0\right)=0, V\left(0\right)=\frac{1}{\sqrt{1+\mu^2}}, \tag{15a}$$

$$U\left(z_\delta\right)=\frac{\mu}{\sqrt{1+\mu^2}}, V\left(z_\delta\right)=0, W\left(z_\delta\right)=-\frac{\mu}{\sqrt{1+\mu^2}}z+C, \tag{15b}$$

where C is some constant to be determined, P_r is the radial pressure distribution on the disc given from the potential flow moving perpendicularly to a disc, and z_δ is the dimensionless boundary layer thickness.

These substitutions and the resulting equations reduce (with slight modifications) to the ones used by von Karman [1] for $\mu=0$ and the ones used by Hannah [6] only for favourable pressure gradients (windward side of disc when $\mu\neq 0$).

But the problems of flow separation on the leeward side of disc still remain unclear even for steady incompressible flow, and conceptual confusion and controversy often appear in the literature [9].

The numerical solution of (11)-(14) subjected to (15a) and (15b) is relatively straight-forward, e.g. by a shooting method where (15a) provides three initial conditions, with two more initial conditions $U'\left(0\right)$ and $V'\left(0\right)$ chosen iteratively until (15b) has been satisfied at a

suitable large finite value of z (z_δ) to within some prescribed accuracy. The equation (14) integrates immediately to give

$$P_z = W' - \frac{1}{2}W^2, \tag{16}$$

since $P_z = 0$ when W, W' vanish.

Flow of non-viscous fluid. When viscosity is ignored, the solution will be the same for a rotating as for a stationary disc since the rotation of the disc only affects the fluid velocity through the viscous drag which it exerts.

The solution of the inviscid irrotational flow can be found by the conformal mapping technique from the streaming motion past a planetary ellipsoid [12]. This stream function for the impinging flow in a circular disc is

$$\Psi = \frac{W_{*\infty} R_*^2}{\pi}\left[\sinh\xi - \cosh^2\xi \cot^{-1}(\sinh\xi)\right]\sin^2\eta, \tag{17}$$

where Ψ is the stream function solution, $z_*/R_* = \sinh\xi\cos\eta$ and $r_*/R_* = \cosh\xi\sin\eta$. Using the solution (17), the velocity are obtained as

$$v_{*r} + iv_{*z} = \frac{1}{r_* R_* \cosh(\xi + i\eta)}\left(\frac{\partial\Psi}{\partial\xi} - i\frac{\partial\Psi}{\partial\eta}\right) - iW_{*\infty}, \tag{18}$$

and after a few calculation we obtain

$$\begin{aligned} v_{*r} &= \frac{2W_{*\infty}R_*}{\pi r_*}\frac{\cos\eta\sin^2\eta}{\cos^2\eta + \sinh^2\xi}, \\ v_{*z} &= \frac{2W_{*\infty}}{\pi}\left[\cot^{-1}(\sinh\xi) - \frac{\sinh\xi}{\cos^2\eta + \sinh^2\xi}\right] - W_{*\infty}, \end{aligned} \tag{19}$$

On the disc surface we have

$$v_r = \frac{2W_{*\infty}r_*}{\pi\sqrt{R_*^2 - r_*^2}}, v_{*z} = 0, \tag{20}$$

and therefore, the pressure coefficient on the stationary disc is

$$C_p \equiv \frac{p - p_{*\infty}}{\rho/2W_{*\infty}^2} = 1 - \frac{4}{\pi^2}\frac{r_*^2}{R_*^2 - r_*^2}, \tag{21}$$

Vortex structure. The theory reveals that, for laminar flow, once the local behavior of separation and attachment is known, the formation of free vortex layers and the total friction experienced by the body can be completely determined. Due to the engineering interest of flow separation and separated vortical flow associated with rotating discs, the understanding in detail of its structure is necessary.

But, the above mentioned theoretical approaches are not adequate for predicting unsteady flow structures with large-scale separations and 3D flow vortices. Therefore, the Computational Fluid Dynamics (CFD) capabilities are used for getting an insight into the separating flow behind a rotating disc in axial flow.

3. RESULTS AND DISCUSSIONS

3.1 Pressure distribution

In order to solve the similarity equation system (11)-(15), the pressure distribution P_r on the disc must be known. The potential flow solution obtained by means of Eq. (17) is shown in Fig. 2, which contains the streamline pattern (Fig. 2a) and radial pressure distribution on the disc surface (Fig. 2b).

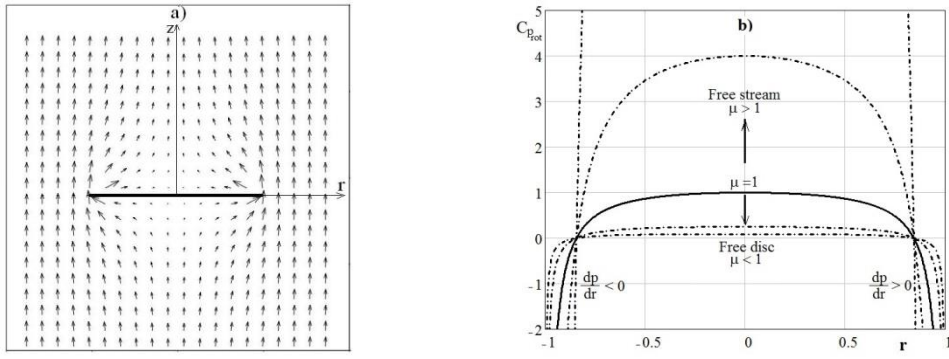

Figure 2 – Potential flow field: a) streamline pattern; b) pressure distribution on stationary and rotating disc

As shown in Fig 2b the radial pressure gradients are favourable on the leading side of disc and flow is attached up to the edge, while on the leeward side of disc the adverse pressure gradient can produce less and more flow separation depending on the value of μ. Using the method of Stratford [14], the laminar separation location does not require the solution of the laminar boundary-layer equations. For a given pressure distribution $C_p(r)$, the expression $C_p^{1/2}\left(rdC_p/dr\right)$ is easy to calculate on the disc. $C_{p_0} = \dfrac{p_0 - p}{\rho/2 \cdot (\Omega R_*)^2}$ is the pressure coefficient on a rotating disc and p_0 is the pressure at the stagnation point, i.e. at the origin. Laminar separation is predicted when it reaches a value of 0.102. Figure 3 shows the location of the separation point depending on the rotation parameter μ which increases approximately linear up ½, $r_s \approx 1 - \dfrac{\mu}{2}$, after that follows a sudden rise, $r_s \approx \dfrac{1}{2\mu}$. As we will further show, the nature of the separation is related to the generation of vortices into the viscous layer adjacent to the disc. The vortex structure differs if the disc is stationary or in rotation.

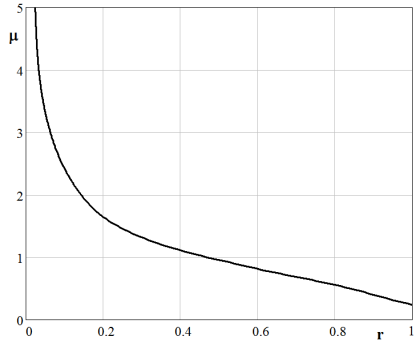

Figure 3 – Laminar separation on the leeward side of disc after Stratford's criterion

3.2 Velocity distribution

The solution of the system of equations (11)-(14) yields velocity distributions near the disc rotating in an axial flow. It is seen from Fig. 5(a, b) that the velocity components *U* and *V* have appreciable values only in a thin layer of thickness $z_\delta = 5$ on the leading side (or windward) of disc and $z_\delta = 10$ on the leeward side of disc. The velocity profiles on the windward side of disc where the flow is subjected to favourable radial pressure gradients are similar with the ones for the case of a free disc (Fig. 5a).

But on the leeward side of disc where there are adverse radial pressure gradients, the 3D boundary layer is subjected to separation beginning from the edge to center as the rotation parameter μ increases (Fig. 4).

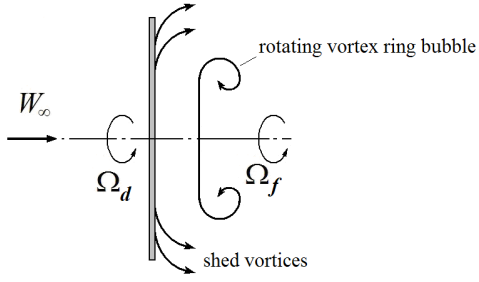

Figure 4 – Boundary layer on a rotating disk in axial flow (on leeward side)

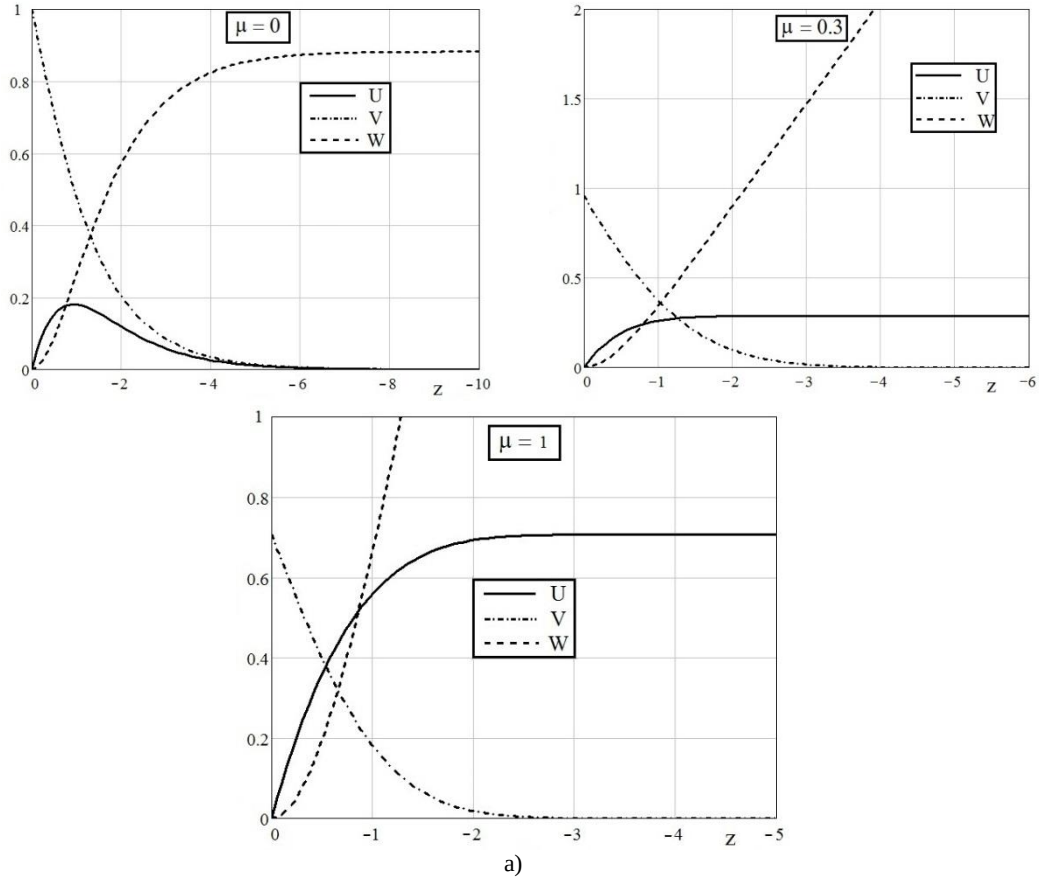

a)

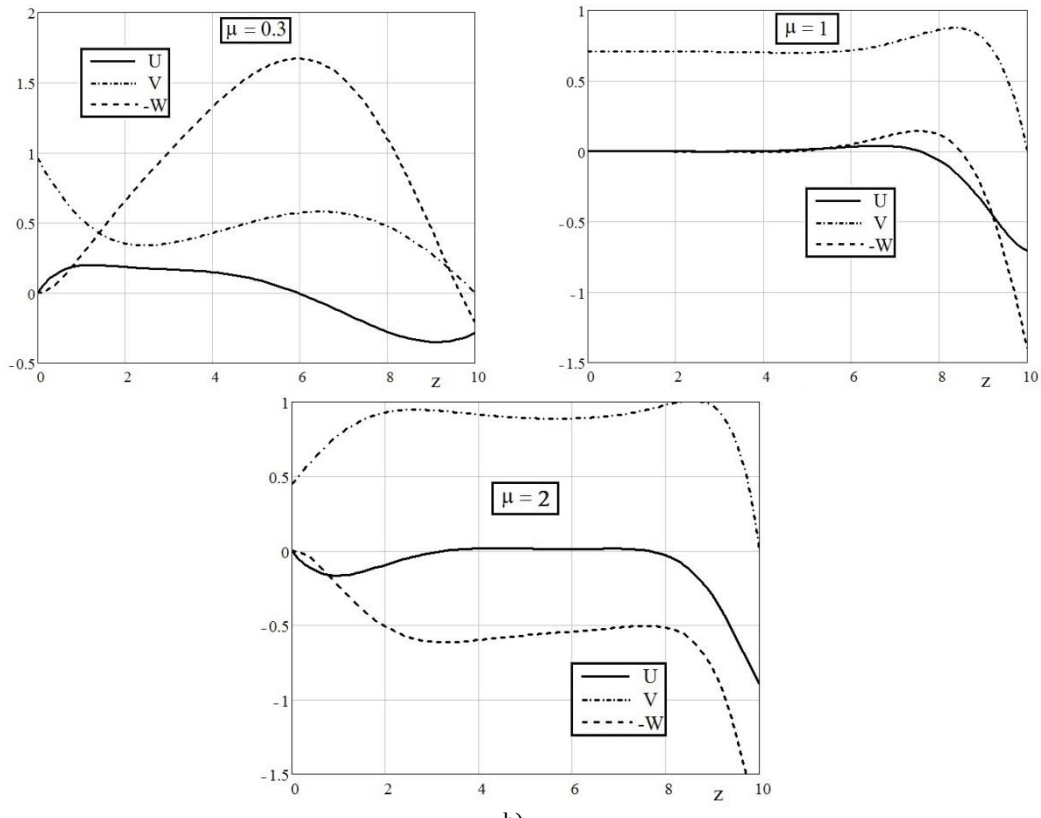

b)

Figure 5 – Velocity distributions in boundary layer: a) on the windward side of the disc b) on the leeward side of the disc

When the boundary layer separates, rotating vortex structures as vortex ring bubbles arise close to the disc, Fig. 4. When μ is small but non-zero, the angular velocity of the vortex ring bubble is smaller than the one of the disc ($V < 1$), the radial flow component U is directed away from the axis of rotation, and the axial flow ($W < 0$) is towards the disc surface, Fig. 5b. The tangential velocity profiles, $V(z)$, point out that the viscous layer in the vicinity of the disc surface contains a thinner sublayer of thickness $z_E = 2$ where fluid and disc co-rotate at almost the same angular velocity like the Ekman layer, followed above by a superlayer of rotational flow essentially inviscid subjected to the Taylor-Proudman theorem. The fluid present in the bottom of separating Ekman layer is thrown outwards and is transported to a vortex ring bubble or Taylor-Proudman flow. This way, an amount of angular momentum is transferred in the Taylor-Proudman flow and the disc acts as a centrifugal fan, a pumping effect occurring. The augmentation of angular momentum continues up to $\mu = 1$, when reaches maximum value at about $\mu \approx 0.3$, after that the angular momentum begins to decrease and in the limit $\mu \to \infty$ we may expect to cancel. When μ is of unity order, the surface shear forces vanish, $(U', V')_{z=0} = 0$, the angular velocity of the fluid is comparable with the one of the disc, and the fluid and disc co-rotate at almost the same angular velocity with no axial flow ($W = 0$) Fig. 5b ($\mu = 1$).

When μ exceeds the value of unity, the angular velocity of the vortex ring bubble is faster than the one of the disc ($V > 1$) similarity to a rotating fluid above a stationary disc [5],

the peripheral fluid flows radially inward through the thin Ekman layer toward the axis, Fig. 5b ($\mu > 1$) ($U < 0$), and the centripetal fluid is replaced by an axial flow outwards the disc surface occurring a suction effect ($W > 0$).

In the limit $\mu \to \infty$, the vortex ring bubble squeezes around the axis of rotation and in this way, the angular momentum of rotating fluid cancels.

Understanding the transport process of angular momentum from a rotating body (there disc) to an uniform superimposed flow of fluid perpendicular to body is important for many engineering applications, one of which could be the vortex rings used for elementary excitations in turbulence. The angular momentum transport measured by the circulation of the boundary layer can be described as a two-step process: generation of vortex ring from separating Ekman shear sublayer when μ increases up to $\mu = 1$, followed by dissipation of angular momentum in the Taylor-Proudman superlayer which is squeezed around the rotation axe according to the law $\Gamma_r \cdot \mu = const.; \Gamma_r$ is the local circulation of the vortex ring bubble which is fixed by the azimuthal velocity component V_0 inside the boundary layer at *z* for $U = 0$: $\Gamma_r = 2\pi r_s V_0$.

Figure 6 illustrates the angular momentum transfer for a rotating disc in axial flow, where the production of circulation occurs on the outer half of that of the disc, with Γ_{max}, for μ=0.3, while on the inner half-disc is its dissipation as μ exceeds unity. The result is in agreement with the well-known Taylor's sphere experiment.

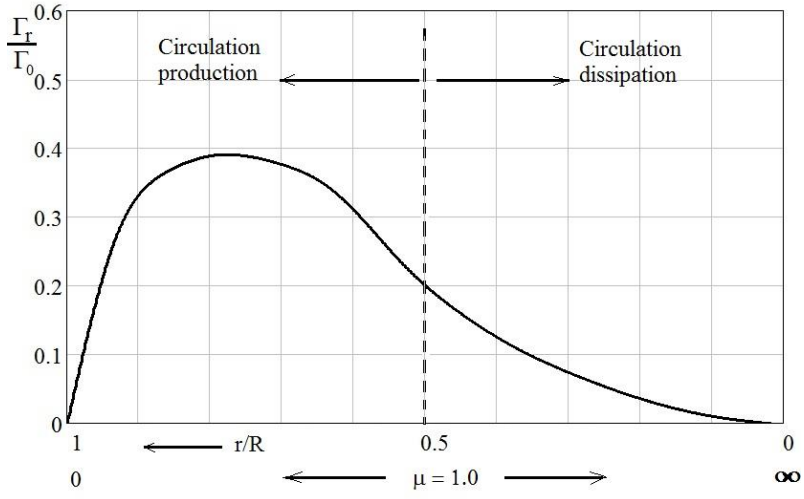

Figure 6 – Circulation of the vortex flow behind the disc

3.3 Streamline pattern

The streamline patterns of the flow behind the disc have been investigated with a numerical code which can provide opportunities to extend the research to topological structures of 3D vortex flow separation shown in Fig. 8.

ANSYS FLUENT [14] was used for the numerical computations of the study.

The computational domain has the far field boundary (half circle) placed at 20*R* from disc (*R*=1 m), and it contains about 10^6 nodes with refinement near to disc (Fig.7). The first layer of cells, near to the wall, has thickness around of 10^{-6}m. The layer is inflated from the disk surface at a growth rate of 1.05.

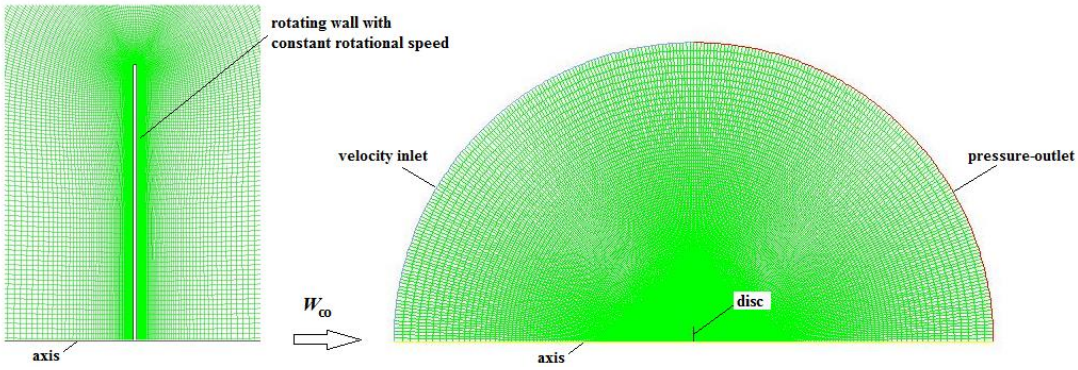

Figure 7 – Disk mesh and computational domain mesh

We considered for computational simulation an axisymmetric swirl laminar flow with the *Oz* as symmetry axis. The undisturbed stream velocity W_∞ is considered parallel with the *Oz* axis and the non-slip condition is selected for disc surface in rotating reference system attached to disc.

A fully unsteady, incompressible pressure-based solver on a second order SIMPLEC algorithm was selected to accurately capture the unsteady flow behaviour. Explanations of the scheme, settings and recommended constants may be found in ANSYS FLUENT 13 documentation [14]. The numerical time step size was set to an equivalent of 1/10 deg rotation of disk. The vortex flow separation is shown in Fig. 8 for two Reynolds numbers, Re_Ω, 10^4 and 10^5. The vortex structures result from the flow separation produced by adverse radial pressure gradients of the leeward side of disc; to describe entrainment one has to employ the term "rotating vortex ring bubble".

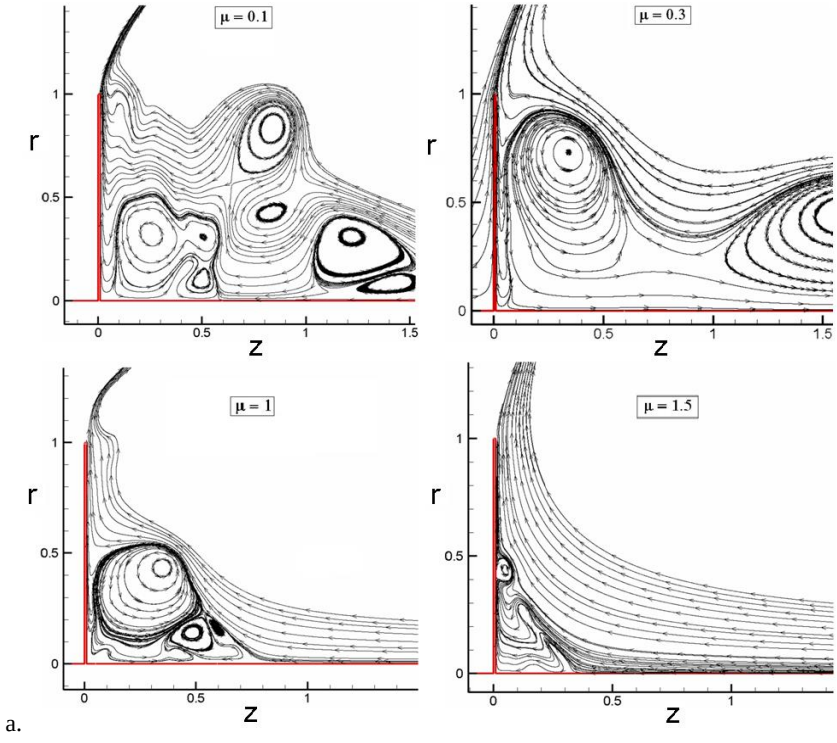

a.

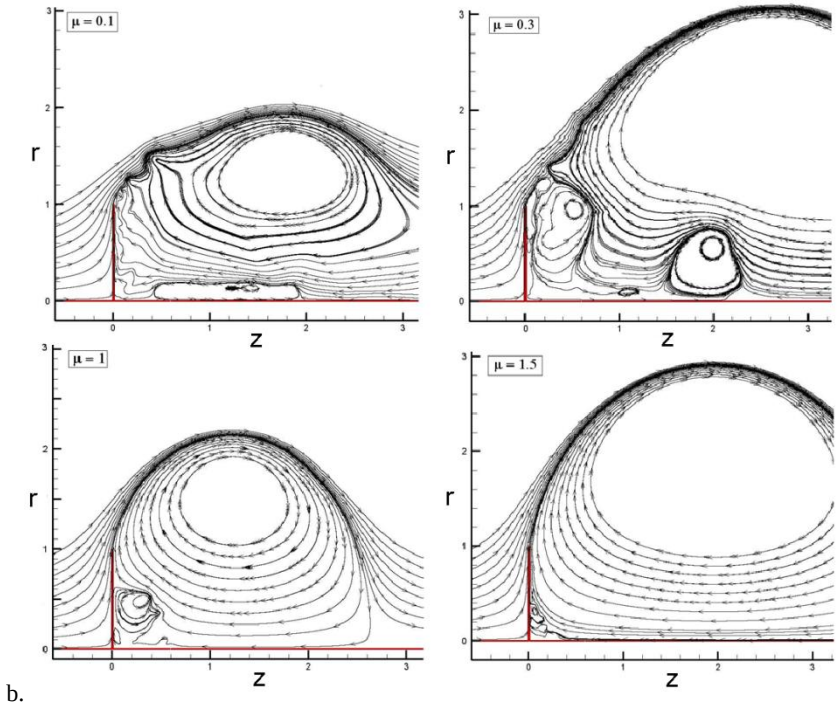

b.

Figure 8 – Streamlines on the leeward side of the disc in the FLUENT calculations for $\mathrm{Re}_\Omega = 10^4$ (a) and $\mathrm{Re}_\Omega = 10^5$ (b)

It refers to the volume of fluid being instantaneously transported with the ring. This concept is precise only for a steadily rotating ring, i.e. it is the volume enclosed by the dividing streamline in a reference frame moving with the ring.

From Fig. 7, it is observed that as μ increases, the circulation of bubble continually increases due to angular momentum transfer from separating Ekman sublayer and its size decreases because its angular momentum has to be shared with a greater angular velocity of fluid. When $\mu = 1$, the angular momentum transfer is maximum, and the fluid and disc co-rotate at almost the same angular velocity.

For $\mu > 1$, both circulation and size of bubble decrease according to the rule $\Gamma_r \cdot \mu = const.$ and $r_b \approx 1/2\mu$.

For $\mu \le 0.3$ the streamlines indicate clearly the Ekman sublayer and Taylor-Proudman superlayer.

But, for the greater values of μ, the simulation model accuracy is limited and it is not able to capture the Ekman layer-flow structure.

3.4. Moment coefficients on the rotating disc

Tifford and Chu [7] obtained solutions to the laminar flow equations for the moment coefficient for impinging flow on a rotating disc at various values of μ, but only for the leading side of disc.

To our knowledge, a solution for the leeward side of disc is lacking. Figure 8 shows a comparison of various solutions for the moment coefficient C_m on both leading side and leeward side of disc.

The present similarity solution for upstream flow has been corrected with edge effect, which implies this solution for the whole disc: $R_*^{'} = \left(1+\mu^2\right)^{-\frac{1}{8}} R_*$ when $\mu < 1$ and $R_*^{'} = 0.9 R_*$ if $\mu \geq 1$.

The corrected similarity solution is in a good agreement with CFD solution. The similarity solution on the leeward side of disc is not in the agreement with the CFD calculations.

The discrepancy between predicted and numerical $C_m = \dfrac{M_*}{1/2 \rho_* \Omega_*^2 R_*^3}$ is due largely to the 2D URANS approach used in the FLUENT code, which cannot model, with sufficient fidelity, the flow structures with large scale separations behind the rotating disc. From Fig. 9 we can also observe the influence of the inertia forces associated with the span motion of the bubble: when $\mu < 1$ the force Coriolis ($C_{f,\theta} = \dfrac{1}{\pi} C_m$) is greater than the centrifugal force in *r* direction, and is acting in the span direction, stabilizing the motion, while when $\mu > 1$, the force Coriolis changes its direction, causing a strong instability effect.

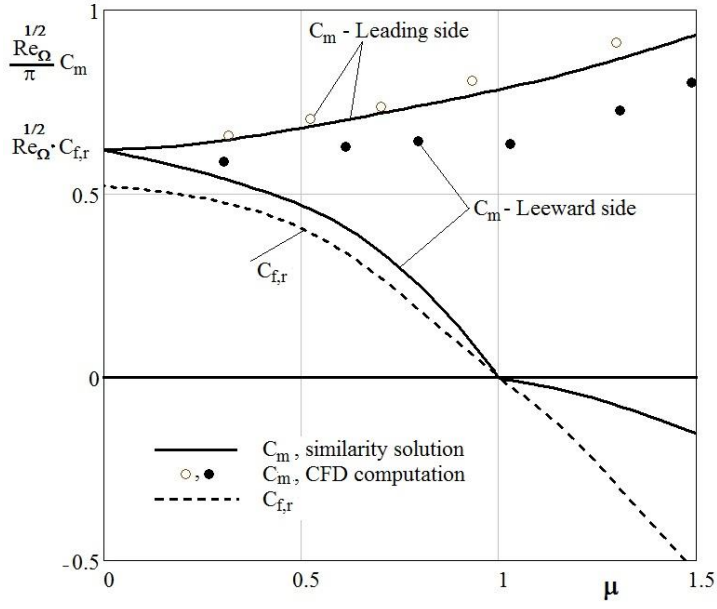

Figure 9 – Moment (C_m) and radial wall shear stress ($C_{f,r}$) coefficients

4. CONCLUSIONS

A physical description has been applied for the laminar uniform superimposed flow of air perpendicular to a rotating disc impinging on the surface. The investigation has been particularly focused on the flow events behind the disc, which has a more general interest by the angular momentum transfer from a rotating rigid body to a steady translation of air parallel to the axis of rotation.

It is shown that the angular momentum of flow behind the disc increases along with μ, reaches a maximum value for μ about 0.3 and tends to zero when $\mu \to \infty$. The maximum transferred value to fluid is of order half of the angular momentum produced by the disc,

$\Gamma_0 = 2\pi R_*^2 \Omega$. As μ increases up to unity, the 3D boundary layer is continually separating on the outboard half of the disc and a rotating vortex ring bubble carrying angular momentum is formed in the vicinity of the disc surface

This is the circulation production step of the transfer process. A circulation dissipation step follows after $\mu = 1$, the circulation decay is according to the law $\Gamma_r \mu = const.$ and the vortex ring bubble squeezes around the axis, and in the limit $\mu \to \infty$ its size and angular momentum cancel. These are the fundamental basic flow characteristics that produce enhanced angular momentum in the rotating-disc boundary layer by an axial flow impinging on the disc surface. The behaviour of the flow leeward the rotating disc is closely related to the stall-delay phenomenon for the horizontal axis wind turbines when the circulation around the inner airfoils of the blade is enhanced at high wind speeds ($\mu = 0.3 - 1.0$) [15].

ACKNOVLEDGMENTS

This work was realized through the Partnership programme in priority domains – PN II, developed through support provided from ANCS CNDI – UEFISCDI, project no. PN-II-PT-PCCA-2011-32-1670.

REFERENCES

[1] Th. von Karman, *Über laminare und turbulente reibung, Zeitschrift für angewandte Mathematik und Mechanik*-ZAMM **1**: pp. 233-252, 1921.

[2] W.G. Cochran, *The flow due to a rotating disc*, Proceedings Cambridge Phil. Society; Vol. **30**: pp. 365-375, 1934.

[3] C. Y. Wang, Exact solutions of steady-state Navier-Stokes equations, *Ann. Rev. Fluid Mech*. Vol. **23**, DOI: 10.1146/annurev.fl.23.010191.001111, pp. 159-177, 1991.

[4] N. Gregory, J. T. Stuart, W. S. Walker, On the stability of three-dimensional boundary layers with application to the flow due to a rotating disc, *Phil. Trans. R. Soc.*, Vol. **A248**, doi: 10.1098/rsta.1955.0013, pp. 155-199, 1955.

[5] U. T. Bödewadt, Die Drahströmung über festen Grunde, *ZAMM Z. Angew. Math. Mech.*, Vol. **20**, pp. 241-253, 1940.

[6] D. M. Hannah, *Forced flow against a rotating disc*, British Aeronautical Research Council Reports and Memoranda, Tech. Rep. 2772, University of Michigan, 1947.

[7] A. N. Tifford, S. T. Chu, On the flow around a rotating disc in an uniform stream, *J. Aeronautical Sciences*, Vol. **19**, pp. 284-285, 1952.

[8] J. M. Owen, R.H. Rogers, *Flow and heat transfer in rotating-disc systems, Vol. 1: Rotor-stator systems*, New York Wiley Taunton Research Studies Press, 1989.

[9] G. K. Batchelor, Note on a class of solutions of the Navier-Stokes equations representing steady rotationally-symmetric flow, *The Quarterly Journal of Mechanics and Applied Mathematics*, Vol. **4**, Online ISSN 1464-3855 - Print ISSN 0033-5614, pp. 29-41, 1951.

[10] V. W. Ekman, On the influence of the earth rotation on ocean currents, *Arkiv. Math. Astro. Fysic.*, Vol. **2**, 1-53, 1905.

[11] L. M. Milne-Thomson, *Theoretical Aerodynamics*, Mc. Millan, London, 1966.

[12] J. J. Healey, Inviscid long-wave theory for the absolute instability of the rotating-disc boundary layer, *Proc. R. Soc. A*, Vol. **462**, Online ISSN: 1471-2946, doi: 10.1098/rspa.2005.1634, pp. 1467-1492, 2006.

[13] B. S. Stratford, *Flow in the laminar boundary layer near separation*, Reports and Memoranda No. 3002 November,1954.

[14] ***, ANSYS Fluent-Commercially available CFD software package based on the finite volume method, www.ansys.com.

[15] H. Dumitrescu, V. Cardos, Inboard stall delay due to rotation, *J. Aircraft*, Vol. **49,** no.1, ISSN: 0021-8669, EISSN: 1533-3868, doi: 10.2514/1.C031329, pp. 101-107, 2012.